

# Amyloid beta deposition related retinal pigment epithelium cell impairment and subretinal microglia activation in aged APPswePS1 transgenic mice

Zhi-Zhang Dong<sup>1</sup>, Juan Li<sup>2</sup>, Yi-Feng Gan<sup>1</sup>, Xue-Rong Sun<sup>3</sup>, Yun-Xia Leng<sup>4</sup>, Jian Ge<sup>5</sup>

<sup>1</sup>The 2<sup>nd</sup> Affiliated Hospital & Yuying Children's Hospital of Wenzhou Medical University, Wenzhou 325200, Zhejiang Province, China

<sup>2</sup>Xi'an No.4 Hospital, Xi'an 710000, Shaanxi Province, China

<sup>3</sup>Institute of Aging Research, Guangdong Medical College, Dongguan 523000, Guangdong Province, China

<sup>4</sup>Guangzhou First Municipal People's Hospital, Guangzhou 510060, Guangdong Province, China

<sup>5</sup>State Key Laboratory of Ophthalmology, Zhongshan Ophthalmic Center, Sun Yat-sen University, Guangzhou 510060, Guangdong Province, China

**Co-first authors:** Zhi-Zhang Dong and Juan Li

**Correspondence to:** Jian Ge. State Key Laboratory of Ophthalmology, Zhongshan Ophthalmic Center, Sun Yat-sen University, Guangzhou 510060, Guangdong Province, China. gejian@mail.sysu.edu.cn

Received: 2017-09-26 Accepted: 2018-03-21

## Abstract

• **AIM:** To identify the pathological role of amyloid beta (A $\beta$ ) deposition in retinal degeneration, and explore A $\beta$  deposition on the retinal pigment epithelium cells (RPE) layer and the associated structural and functional changes in Alzheimer's disease transgenic mice.

• **METHODS:** RPE changes in the eyes of APPswe/PS1 transgenic and none transgenic (NTG) mice over 20 months old were examined. Histological changes were investigated via hematoxylin and eosin (H&E) staining and transmission electron microscopy (TEM) examination, whereas the expression of amyloid precursor protein (APP), A $\beta$ , Zonula occludens-1 (ZO-1) and Ionized calcium binding adaptor molecule-1 (IBA-1) were investigated using immunohistochemistry and immunofluorescence techniques. All of the obtained results were quantitatively and statistically analyzed.

• **RESULTS:** In aged transgenic mice, an APP-positive immunoreaction and A $\beta$  deposition were detected on the RPE layer but were undetectable in NTG mice. The RPE demonstrated some vacuole changes, shortened basal infoldings and basal deposition in histopathological examination and TEM tests, wherein irregular shapes were indicated by ZO-1 disorganization through fluorescence.

Furthermore, IBA-1 positive cells were observed to have accumulated and infiltrated into the RPE layer and localized beneath the RPE/Bruch's membrane (BrM) complex, which was accompanied by an increase in BrM thickness in aged transgenic mice in comparison to NTG mice. The IBA-1 positive cells were found to be co-stained with A $\beta$  deposition on the RPE flat mounts.

• **CONCLUSION:** The observed A $\beta$  deposition in the RPE layer may cause RPE dysfunction, which is associated with microglia cells infiltration into the retina of aged transgenic mice, suggesting that A $\beta$  deposition probably plays a significant role in RPE-related degenerative disease.

• **KEYWORDS:** amyloid beta; retinal pigment epithelium cells; retina; age related macular degeneration; Alzheimer's disease  
**DOI:10.18240/ijo.2018.05.06**

**Citation:** Dong ZZ, Li J, Gan YF, Sun XR, Leng YX, Ge J. Amyloid beta deposition related retinal pigment epithelium cell impairment and subretinal microglia activation in aged APPswePS1 transgenic mice. *Int J Ophthalmol* 2018;11(5):747-755

## INTRODUCTION

Alzheimer's disease (AD) is a progressive neurodegenerative disease that is characterized by memory loss and cognitive deficits in elderly people, commonly older than 65 years of age. This condition is pathologically characterized by amyloid beta (A $\beta$ ) plaque deposits and/or neurofibrillary tangles in the brain<sup>[1-2]</sup>. As a processed product of amyloid precursor protein (APP), A $\beta$  deposits are believed to be neurotoxic to nearby cells and to stimulate an inflammation reaction *in vivo*<sup>[3-5]</sup>. Currently, understanding the impact of A $\beta$  deposits in the eye has been one of the most researched topics in Alzheimer's study. Recently, a significant body of works has appeared investigating A $\beta$  deposition and A $\beta$ -related retinal degenerative changes in the retinas of AD transgenic mice models<sup>[6-7]</sup>, and A $\beta$  plaque deposition has been detected in the retinas of these different AD transgenic mice models<sup>[8-9]</sup>. According to these studies, A $\beta$  deposition causes both functional and structural retinal abnormalities; however, little is known regarding A $\beta$  depositions and A $\beta$ -related pathological degeneration in the retinal pigment epithelium cells (RPE) layer in these AD transgenic mouse models.

Age-related macular degeneration (AMD) is a degenerative retinal disease that causes irreversible vision loss in the elderly, and the RPE cell monolayer is observed to play a critical role in this disease<sup>[10-11]</sup>. A $\beta$  peptides have been found in RPE cells and drusen in AMD patients<sup>[12-14]</sup>. At the same time, Bruban *et al*<sup>[15]</sup> reported that subretinal A $\beta$  injection causes RPE cell alterations and dysfunctions that lead to retinal degeneration in mice<sup>[16]</sup>. Furthermore, Yoshida *et al*<sup>[17]</sup> had suggested that A $\beta$  might be responsible for the pathogenesis of AMD by causing RPE degeneration. Although some mechanisms have been suggested for RPE degeneration due to A $\beta$  deposition, including inflammatory events<sup>[18-19]</sup> and A $\beta$  cellular toxicity, the definite pathogenesis of A $\beta$  in relation to RPE degeneration in the retina has yet to be elucidated.

As well known, A $\beta$  deposition could activate microglia cells in the brain, and activated microglia cells might attempt to clear A $\beta$  at the possible expense of an inflammatory overreaction<sup>[20]</sup>. Recently, the accumulation of activated microglia cells in the subretinal space was suggested to be associated with structural and functional changes in the RPE<sup>[21-22]</sup>. In retinas of AD transgenic mouse models, it remains unclear as to whether microglia cells are involved in A $\beta$  deposition-induced RPE degeneration *in vivo*.

By using APPswePS1 transgenic mice, which is an established double transgenic AD mouse model with a Swedish APP mutations (APPswe) and a mutant human Presenilin1 (PS1), we sought to further elucidate the mechanism of A $\beta$  deposition-associated RPE degeneration. In this study, we characterized the expression of APP and A $\beta$  deposits in addition to microglia cell activation in the RPE layer of APPswePS1 transgenic mice.

## **MATERIALS AND METHODS**

**Animal Treatment** The APPswePSEN1dE9 transgenic (APP/PS1) mice and non-transgenic littermates (NTG) were obtained from Jackson Laboratory, Bar Harbor, ME, USA<sup>[23]</sup>. For this study, 24 APP/PS1 and NTG mice (12 of each kind) were used, and these mice were at least 20 months old. All of the mice that were used in our experiments were tested and verified not to have the retinal degeneration 1 mutation (Pde6b<sup>rd1+</sup>)<sup>[24-25]</sup>. Before the experiments, the mice were housed in a 12-hour light/12-hour dark cycle with food and water *ad libitum*. All animal procedures were conducted in accordance with the guidelines established by the ARVO Statement for the Use of Animals in Ophthalmic and Vision Research and with Institutional Animal Care and Use Committee (IACUC) protocols. Experimental protocols were also approved by the animal ethics committee of the 2<sup>nd</sup> Affiliated Hospital & Yuying Children's Hospital of Wenzhou Medical University.

**Histopathology** Tissue histology was performed as described before<sup>[9,22]</sup>. Each mouse was deeply anesthetized with an overdose of 4.3% chloral hydrate (0.1 mL/g) and was transcardially perfused with 30 mL of ice-cold 0.1 mol/L

phosphate-buffered saline (PBS), pH 7.4. The eyes of each mouse were enucleated and fixed in 4% paraformaldehyde (PFA) in PBS (pH 7.4) overnight at room temperature (RT). The eyes were dehydrated in a series of isopropanol concentration (70%, 90% and 100%), and subsequently embedded in paraffin. Next, the eyes were subjected to histopathology. The eyes were serially sectioned through the pupillary-optic nerve to a 4- $\mu$ m thickness, and the sections were either stained with hematoxylin and eosin (H&E; Sigma, St. Louis, MO, USA) or were further prepared for immunocytochemistry analysis. These sections were examined *via* light microscopy in which images were collected from areas that were approximately 300-500  $\mu$ m away from the optic nerve.

**Immunocytochemistry** As described in previous study<sup>[19]</sup>, for the immunohistochemical analysis, the sections were deparaffinized, rehydrated and incubated with 70% formic acid in 0.1 mol/L PBS for 5min at RT for epitope antigen retrieval. After being rinsed with PBS 3 times, the sections were then treated with 3% H<sub>2</sub>O<sub>2</sub> for 20min at RT to eliminate endogenous peroxidase activity. In order to block nonspecific immunoreactivity, the sections were blocked with 5% goat serum in PBS that contained 0.1% Triton X-100 and 20 mmol/L L-lysine for 60min at RT. The sections were then incubated with the primary antibody which was diluted with a primary antibody dilution (Boster, Wuhan, China) at 37°C for 1h. The mouse anti-Alzheimer precursor protein A4 monoclonal antibody (APP) from Chemicon was reacted with 22C11 (1:100). After being rinsed 3 times with PBS for 5min, the sections were additionally incubated with biotinylated goat anti-mouse second antibody (1:1000; Vector Laboratories, Burlingame, CA, USA) for 1h and were consequently incubated with an avidin-biotin-peroxidase complex for 30min (1:100; Vector Laboratories). Washed with PBS, the sections were treated with AEC (Vector AEC substrate kit; Vector Laboratories) according to the manufacturer's instructions and were counterstained with hematoxylin. The intensity of the APP was calculated using Image Pro-Plus5 software (Media Cybernetics Incorporation, USA) in which data were obtained from 3 unconnected corresponding sections through the optic nerve in each mouse in each group. These observations were conducted by observer blinded to the sample information.

**Immunofluorescence** As described by previous work<sup>[15,26]</sup>, for the RPE/choroid flat mounts, the enucleated eyes were sectioned at the equator, and the anterior half, including the lens and vitreous, was discarded. The retinas were carefully peeled from the eyecup under a biomicroscope. The posterior eye segment that contained the RPE/choroid complex was dissected into quarters by eight radial cuts. For the RPE flat mount preparation, eyes were fixed in 4% PFA for 15 to 30min at RT (for A $\beta$  detection, the flat mounts were treated with 70% formic acid for 5min and were washed with PBS

3 times at RT). The RPE/choroid flat mounts were incubated in PBS/bovine serum albumin (BSA) 4%, permeabilized in 0.1% Triton X-100 for 30min and stained with selective primary antibodies in a primary antibody dilution (Boster, Wuhan, China) overnight at 4°C. The antibodies were mouse anti-APP (1:100; Chemicon, USA), mouse monoclonal anti-Zonula occludens-1 (ZO-1; 1:100; Zymed, USA), mouse anti-A $\beta$  monoclonal antibody (1:100; 6E10, Covance, USA), as well as the rabbit polyclonal antibody CP290A for ionized calcium binding adaptor molecule-1 (IBA-1; 1:100; Biacare, Concord, CA, USA). After washing with PBS for 30min, the flat mounts were incubated with a second antibody goat anti-mouse Cy3 or FITC-conjugated IgG (1:100; PTG, China) or a goat anti-rabbit Cy3-conjugated IgG (1:100; PTG, China) along with 4'-6-diamidino-2-phenylindole (DAPI). Next, the flat mounts were mounted and examined under a Zeiss LSM510 laser confocal microscope. For the A $\beta$ - and IBA-1-positive cell quantifications, we randomly selected 4 fixed areas (0.05 mm<sup>2</sup>) of the flat mounts ( $n=6-8$  in each group) and imaged these areas at a magnification of 400 $\times$  approximately 400-500  $\mu$ m away from the optic disc. Next, an observer who was blinded to the group information measured the A $\beta$  plaque immunoreaction intensity using Image Pro Plus5 software in which the observer counted all of the observable IBA-positive cells with dendrite-like morphologies on the RPE layer and beneath the RPE/Bruch's membrane (BrM) interface complex. For morphometric analysis, the perimeters of 400 cells (five different images) obtained from each eye were manually traced in Image Pro Plus5 software in which areas, perimeters, the shape factors [ $4\pi A/P^2$  (A=area, P=perimeter)] approaching 1 corresponded to a more circular/regular cell, for the ideal hexagonal cell shape (hexagon shape factor, HSF;  $P^2/A-13.856$ , A=area, P=perimeter), the value is zero for hexagon and higher value for increased pleomorphism<sup>[27]</sup>, and the cellular degree of elongation (DE) [(Diameter<sub>max</sub>-Diameter<sub>min</sub>)/(Diameter<sub>max</sub>+Diameter<sub>min</sub>)] were calculated as previously described<sup>[28-29]</sup>.

**Transmission Electron Microscopy** For the ultrastructural examination, as previously reported<sup>[22,30]</sup>. Eyes were fixed in 2.5% glutaraldehyde and 1% PFA in 0.1 mol/L sodium cacodylate-HCl (pH 7.4) for at least 24h at 4°C, the eyes were dissected at the level of the limbus, the posterior eyeballs were post-fixed in 1% osmium tetroxide in 0.1 mol/L cacodylate buffer-HCl (pH 7.4) for 4h and the eyes were subsequently dehydrated in increasing concentrations of ethanol (50%, 75%, 95% and 100%) and were infiltrated overnight with a 1:1 propylene oxide mixture. Ultrathin (70-nm thick) sections were fabricated in the samples approximately 0.5 mm away from the optic nerve *via* a Leica Ultracut S microtome (Reichert Ultracut E, Leica). After ultrathin sections were contrasted with uranyl acetate and lead citrate, the samples were observed

under an electron microscope (model 100 CX II, JEOL, Tokyo, Japan) at 80 kV, and the images were captured by an observer blinded to the sample information. Micrographs of 6 eyes from each group were taken from each ultrathin section at various locations, recorded, and they were analyzed to determine the BrM thickness for each eye.

**Statistical Analysis** In all of the graphs that include error bars, the data were represented as means $\pm$ SEM from all individuals in each group of animals ( $n=6-8$ ). The APP/PS1 and NTG groups were compared using Student's *t*-test in SPSS 19 software. A value of  $P\leq 0.05$  was considered to be statistically significant.

## RESULTS

**Accumulation of APP Expression and A $\beta$  Deposition in the RPE Layers of Aged APP/PS1 Mice** Previous studies<sup>[8-9]</sup> have observed A $\beta$  deposition in the retinal ganglion cell (RGC), inner plexiform layer (IPL), outer nuclear layer (ONL), and sclera layer. However, few researchers have reported A $\beta$  deposition in the RPE cell layer in AD transgenic mice. In order to investigate APP expression and its processed product (A $\beta$ ) distribution, we first evaluated the immunoreactivity of APP protein following the reaction of an APP-specific antibody with 22C11 in RPE sections. Consistent with the results of a previously published study<sup>[31]</sup>, APP immunoreactivity was predominantly detected *via* a diffuse pattern in the cytoplasm of RPE cells obtained from APP/PS1 mice both in fluorescein test (Figure 1A) and immunocytochemistry examination (Figure 1C). In contrast, a low level of background APP staining was observed in RPE obtained from NTG mice (Figure 1B, 1D). APP expression quantification revealed 2.342 $\pm$ 0.189 fold changes in APP/PS1 mice in comparison to the NTG group (Figure 1E;  $P<0.001$ ). An identical trend of APP expression is confirmed by fluorescein test. Furthermore, examination of the A $\beta$  immunoreactivity on the RPE flat mounts that were obtained from APP/PS1 mice, which were labeled with an A $\beta$ -specific antibody, 6E10, revealed a remarkable accumulation of A $\beta$  deposits exhibiting a senile plaque-like pattern, as has already been reported in mouse eyes (Figure 1F)<sup>[8-9]</sup>; however, RPE flat mounts that were obtained from NTG mice exhibited almost no detectable reactivity with this A $\beta$  antibody (Figure 1G). More importantly, to ensure that the A $\beta$  deposition was not caused by a nonspecific reaction of a second antibody, we performed an immunostaining with another monoclonal antibody, BAM01 (Neomarker, Fremont, CA, USA), which demonstrated a staining pattern that was similar to that achieved with 6E10 (data not shown). Quantification of the A $\beta$  immunoreactivity on the RPE flat mounts indicated a significant robust A $\beta$  deposition in the RPE layers of aged APP/PS1 mice (Figure 1H), however, we did not further confirm this tendency with Western blotting in APP/PS1 mice.

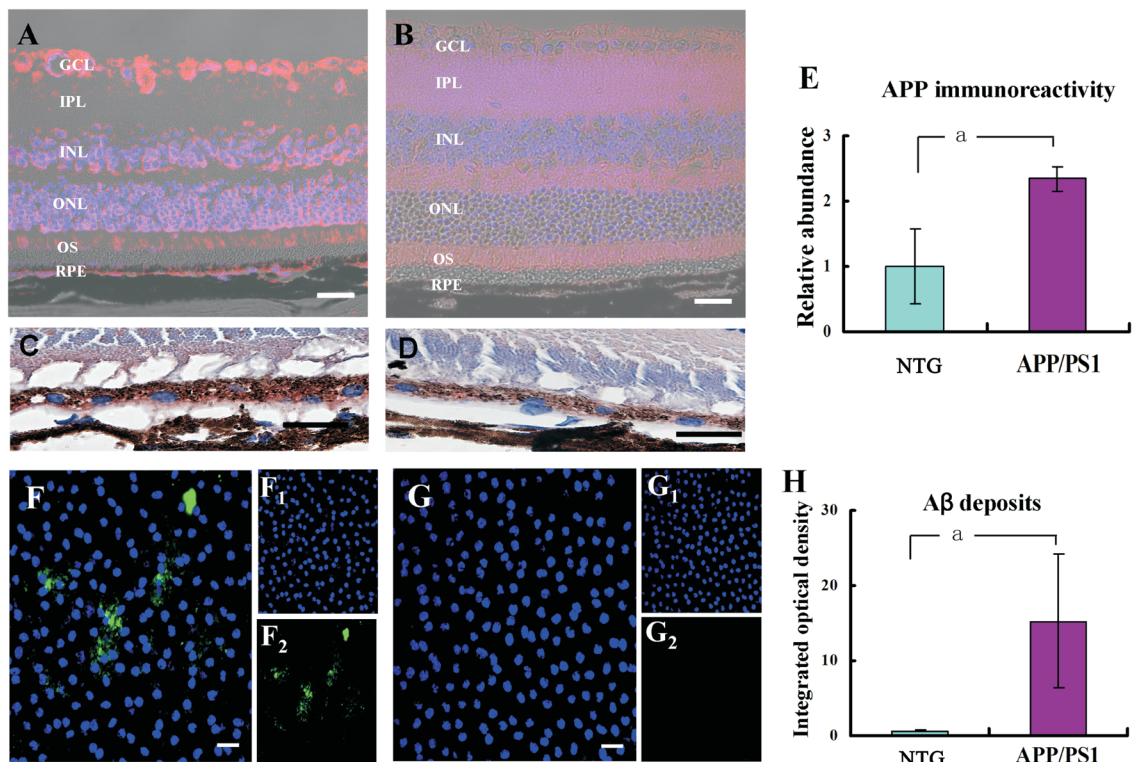


**Figure 1** APP expression and A $\beta$  deposition in the RPE layers of aged APP/PS1 mice Immunofluorescence microscopy revealed the APP expression in the whole retinal sections from APP/PS1 (A) and NTG (B) mice; and the AEC staining revealed the expression of transgene APP protein in RPE from APP/PS1 (C) and NTG (D) mice, respectively. The depicted histogram displays the increase of the APP immunoreaction in APP/PS1 mice (E). Immunofluorescence microscopy revealed A $\beta$  deposition in RPE layers obtained from APP/PS1 mice (F) and NTG (G), (F<sub>1-2</sub>, G<sub>1-2</sub>, respectively). Separate channels for DAPI (blue) and 6E10 staining (green). The difference of A $\beta$  deposition between the NTG and APP/PS1 groups reached statistical significance (H). RGC: Retinal ganglion cell; IPL: Inner plexiform layer; INL: Inner nuclear layer; ONL: Outer nuclear layer; OS: Outer segment; RPE: Retinal pigment epithelium. Error bars=Means $\pm$ SEM; Scale bars=20  $\mu$ m. <sup>a</sup> $P$ <0.001.

**RPE Degeneration in Aged APP/PS1 Mice** Some reports<sup>[8,32-33]</sup> have established that A $\beta$  peptides or depositions could cause the observed retinal degeneration, and because we detected A $\beta$  deposition in the RPE layers of APP/PS1 mice, we further examined RPE structural changes in APP/PS1 mice. The H&E-stained retinal/RPE sections were histopathologically investigated *via* light microscopy and demonstrated almost normal structure in retinal section but with a significant number of vacuoles in the RPE layer (Figure 2A). In contrast, no such change was detected in the RPE layer from NTG mice (Figure 2B). These data suggested a possibility in structural change of the RPE layer. In order to confirm these results, we further examined the RPE/BrM interface using transmission electron microscopy (TEM). Aside from vacuoles that contained membranous material indicated with vacuoles, we identified other degenerative changes in the RPE of APP/PS1 mice, including shortened basal infoldings and basal deposits with electron-dense material above the BrM (Figure 2C). In contrast, the NTG mice displayed a regular RPE/BrM organization without these changes (Figure 2D).

ZO-1 is a membrane adherence junctional protein that help maintaining the barrier junctional integrity of the blood-retinal barrier<sup>[34]</sup>. ZO-1 could serve as a RPE functional and structural

indicator<sup>[15,28]</sup>. Therefore, we investigated RPE damage in APP/PS1 mice by immunostaining RPE flat mounts with ZO-1 antibody. In these mounts, the RPE cell exhibited an irregular shape with a loss of its typical cobblestone-like morphology (Figure 2F). To quantify these changes in RPE cells, the RPE cell size, integrity, and regular shape factor were calculated using Image Pro Plus5 software, and the flat-mount images obtained from all of the groups were manually plotted for calculating the perimeter/area/diameter of each RPE cell (Figure 2G), similarly to that reported by Ding *et al*<sup>[27]</sup>. In the NTG mice, the RPE cell exhibited a regular and well organized structure (Figure 2E). By contrast, the RPE cells displayed a smaller cell size, as indicated by a reduced area in APP/PS1 mice (Figure 2H;  $P=0.0795$ ). The disorganized morphology of RPE cell in APP/PS1 mice was confirmed by specific parameters, such as becoming longer with a significant increase in elongation degree (Figure 2I;  $P<0.0001$ ), losing hexagon shape with an increase value in hexagon shape factor (Figure 2J;  $P<0.0001$ ) and becoming irregular with a significant decrease value in the shape factor (Figure 2K;  $P=0.00216$ ). All of these parameters suggest that the RPE cell becomes much more irregularly shaped in APP/PS1 mice. At the same time, we also found that the presence of ZO-1 was

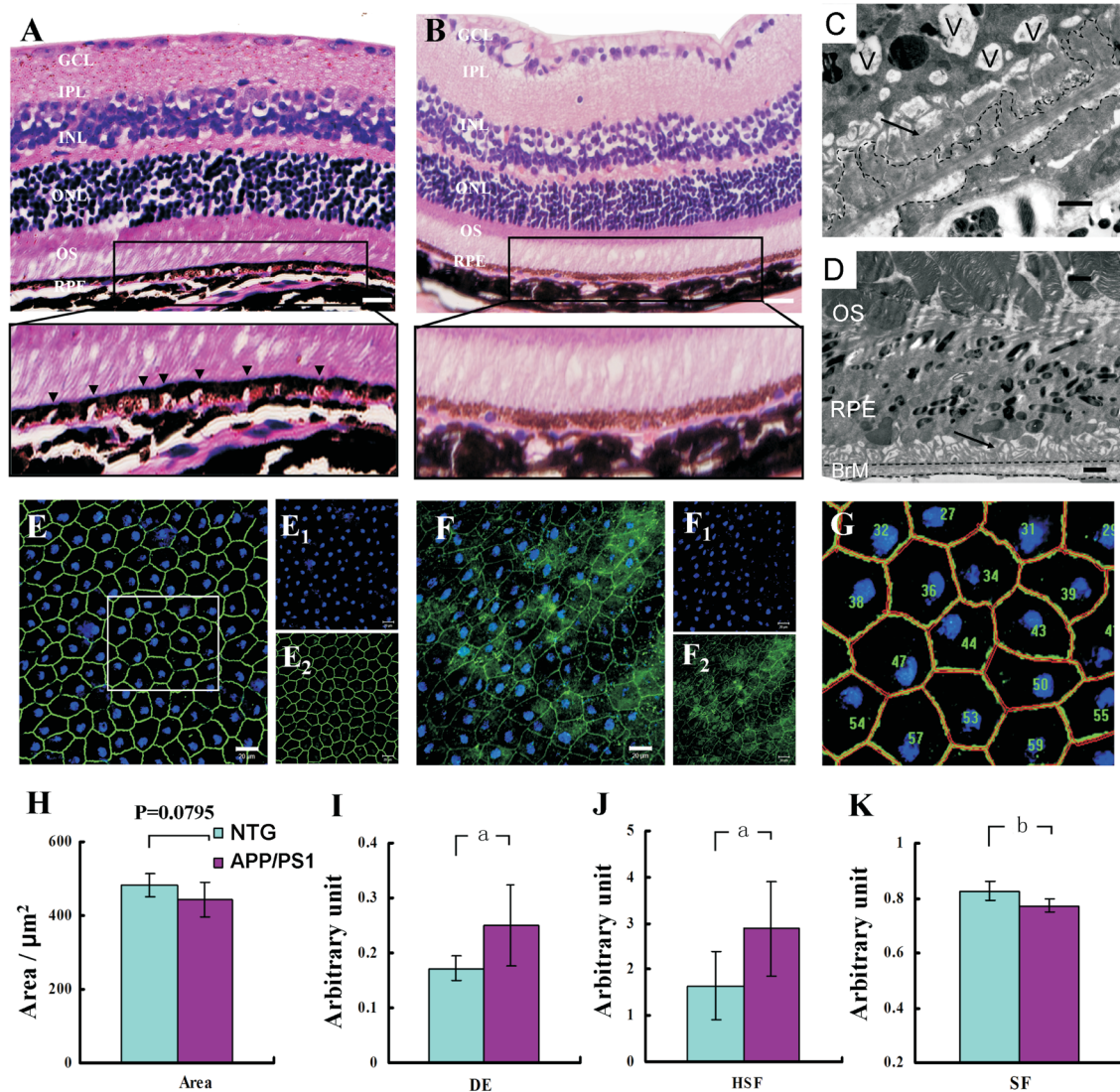


**Figure 2 The RPE morphological degeneration in aged APP/PS1 mice** Histological H&E-stained sections of the RPE layer revealed a large number of vacuoles in APP/PS1 mice (A, arrow head), and no changes in the NTG mice (B), while a higher magnification showed from the rectangle in A, B. Transmission electron microscopy images revealed degeneration changes in APP/PS1 mice (C), including vacuoles (V), shortened basal infoldings (arrow) and basal deposits (black dotted line), while no such change in NTG mice (D). The immunofluorescence staining of ZO-1 on RPE flat mounts exhibited a regular, well-organized structure in NTG mice (E), whereas an irregular disorganization was observed in APP/PS1 mice (F) ( $E_{1,2}$ ,  $F_{1,2}$ ). Separate channels for DAPI and ZO-1. As a higher magnification of E in a sampled rectangle, G was segmented to highlight the method for evaluating the RPE cells morphology change in Image Pro Plus5 software. In a morphometric analysis, the resultant histograms demonstrated a decrease in cell area (H,  $P=0.0795$ ), an increase value in degree of elongation (I), an increase value in hexagon shape factor (J), and a reduce value in shape factor (K) in APP/PS1 mice with. RGC: Retinal ganglion cell; IPL: Inner plexiform layer; INL: Inner nuclear layer; ONL: Outer nuclear layer; OS: Outer segment; RPE: Retinal pigment epithelium; BrM: Bruch membrane. Error bars=Means±SEM; Scale bars=20  $\mu\text{m}$  (A, B, E, F), =1  $\mu\text{m}$  (C, D).  $aP<0.001$ ,  $bP<0.05$ .

not disrupted or even missing in the RPE cell border. The ZO-1 cytoplasmic level exhibited a tendency of increasing; however, we did not further confirm this tendency with Western blotting in APP/PS1 mice.

**Accumulation and Infiltration of IBA-1 Positive Cells in RPE Flat Mounts in Aged APP/PS1 Mice** Recently,  $A\beta$  deposition has always been identified to cause an inflammatory response that can be characterized by the infiltration of microglia in both the brain and retina<sup>[8]</sup>. In order to evaluate glial activity in response to  $A\beta$  deposition in the RPE, we examined the expression of IBA-1, which is a microglia cell

marker, and performed a quantitative analysis in APP/PS1 mice. Figure 3 depicts representative microphotographs of IBA-1 immunoreactivity on RPE flat mounts. Using fluorescent microscopy, a similar pattern of IBA-1 immunoreactivity was detected on RPE flat mounts that were obtained from both NTG and APP/PS1 mice; however, the IBA-1-positive cells in APP/PS1 mice displayed a considerably more “dendritic-like” appearance in comparison to those observed in NTG mice (Figure 3A, 3B). In addition, there was a slight increase in the number of IBA-1-positive cells on the RPE flat mounts in the APP/PS1 group relative to the NTG group, but this

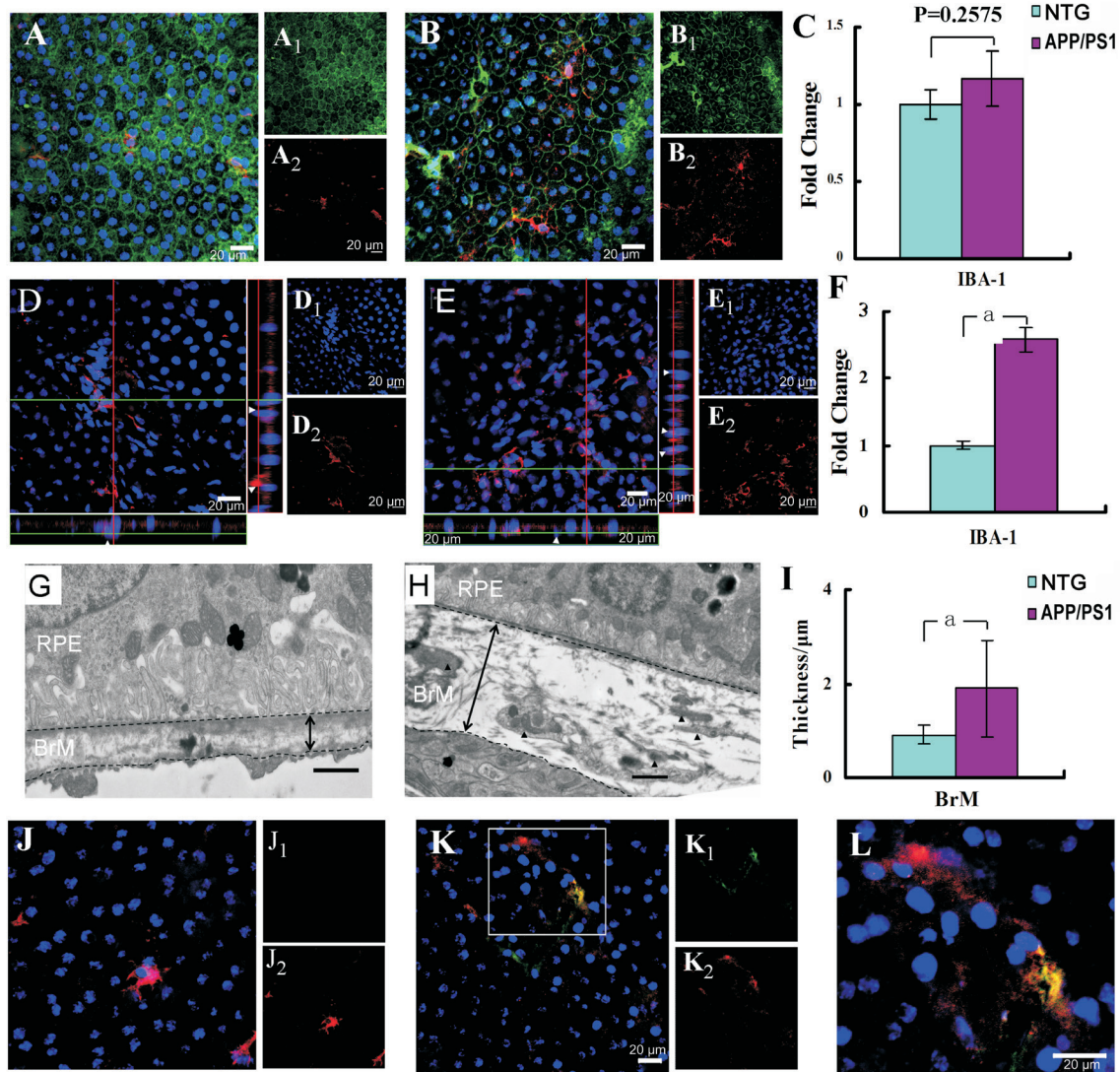


**Figure 3** The accumulation of IBA-1 positive cells on the RPE flat mounts and beneath the RPE/BrM interface complex in aged APP/PS1 mice. A, D, G, J and B, E, H, K, L came from NTG and APP/PS1 mice respectively. Confocal immunofluorescence images depicting IBA-1 (red) and ZO-1 (green) that were detected on RPE flat mounts obtained from NTG (A) and APP/PS1 mice (B). The depicted histogram showed an increase in IBA-1 positive cells on RPE flat mounts, but with no statistical significance (C,  $P=0.2575$ ). D, E demonstrated the IBA-1 positive cells beneath the RPE layer elucidated in the Z-stack (triangle), and the green/red line indicated the Z-stack scanning surface (D, E). The graph in F revealed an increase in IBA-1-positive cells beneath the RPE layer. Transmission electron micrograph of the RPE/BrM interface came from NTG (G) and APP/PS1 mice (H). Some cells can be observed (triangle), the thickened BrM was indicated with a double-headed arrow; I: The thickness of the BrM in APP/PS1 mice was greater than that in NTG mice; J, K: The images were overlaid with L at a higher magnifications of K (in rectangle), indicating IBA-1 positive cells co-stained with A $\beta$  deposition (A-B<sub>1-2</sub>, D-E<sub>1-2</sub>, J-K<sub>1-2</sub>). Separate channels for each staining. RPE: Retinal pigment epithelium; BrM: Bruch membrane. Error bars=Means $\pm$ SEM; Scale bars=20  $\mu$ m (A-E, J-L), 1  $\mu$ m (G, H). <sup>a</sup> $P<0.001$ .

finding was not statistically significant (Figure 3C, Student's *t*-test,  $P=0.2575$ ). Surprisingly, we observed the accumulation of IBA-1 positive cells beneath the RPE layer, as indicated by the nuclei location in the Z-stack and the green/red line that indicated the Z-stack scanning surface (Figure 3D, 3E). Quantification of the IBA-1-positive cells beneath the RPE layer demonstrated a significant increase in the number of IBA-1 positive cells in the APP/PS1 mice, in addition to 2.578 $\pm$ 0.180 fold changes observed in comparison to the NTG group (Figure 3F;  $P<0.0001$ ). This finding was further confirmed by TEM. Electron micrographs revealed abundance of cells under or in the BrM (Figure 3G, 3H) which displayed

almost the same appearance as the IBA-1 positive cells that were found beneath the RPE layer in RPE flat mounts by fluorescence (Figure 3D, 3E). The cells detected in the TEM were associated with the observed thickened BrM (1.896 $\pm$ 1.036  $\mu$ m in the APP/PS1 group vs 0.916 $\pm$ 0.195  $\mu$ m in the NTG group). More importantly, we also found that the IBA-1 positive cells (red color for IBA-1) were co-stained with A $\beta$  deposition (green color for 6E10) in the APP/PS1 mice (Figure 3J, 3K), which indicated that the IBA-1 positive cells contained A $\beta$  peptides; however, not all of the A $\beta$  depositions were surrounded or overlaid with microglia cells, as demonstrated in Figure 3L.

## DISCUSSION

In this study, we focused on the APP and the process product-A $\beta$  depositions, and we investigated the effect of A $\beta$  deposition in the RPE layer in APP/PS1 transgenic mice. We identified the expression of APP and the accumulation of A $\beta$  depositions in the RPE layer, and we demonstrated RPE degeneration that was associated with microglia cells activation and accumulation in the RPE layer in aged APP/PS1 mice.

In this study, we used APP/PS1 transgenic mice, which included a human APP with Swedish mutations (K595N/M596L) and a mutant human presenilin 1 (PS1-dE9). According to previous studies<sup>[35-36]</sup>, overexpression of APP resulted in A $\beta$  deposits in the brain at the age of approximately 6-7mo and in the retina at the age of approximately 12mo<sup>[8,31]</sup>. In our research, RPE cells demonstrated a moderate expression of APP in the cytoplasm of the RPE sections, which was consistent with results reported by previously<sup>[31,37]</sup>. We also found plaque-like A $\beta$  deposits on the RPE flat mounts. Although other researchers had reported senile plaque or A $\beta$  deposition in the retina<sup>[9]</sup> in AD transgenic mouse model, this study reported plaque-like A $\beta$  depositions in the RPE layer on flat mounts from AD transgenic mice. As well-known, RPE cells differ from neuron cells, such as RGC, and RPE cells could phagocytose waste materials or debris originating from the outer segments of photoreceptor cells. It was interesting to recognize that A $\beta$  peptides deposited on the outer segments layer in both human and mouse retinas<sup>[14]</sup>, and that A $\beta$  plaques were also found in the photoreceptor outer segment layer<sup>[9]</sup>, which was also identified in our research (data not shown). These data indicated that the A $\beta$  depositions observed on the RPE flat mounts might have come from photoreceptor cells. On the other hand, Yoshida *et al*<sup>[17]</sup> had suggested an RPE origin for A $\beta$  peptides because of the expression of neprilysin and  $\beta$ -secretase<sup>[38]</sup> in RPE, which was supported by the fact that endoplasmic reticulum (ER) calcium disruption could induce A $\beta$  accumulation in ARPE19<sup>[39]</sup>. Taking these results into consideration, it would be interesting to investigate in further studies where the A $\beta$  peptides/depositions in RPE cells originate.

Furthermore, we identified RPE histopathological degeneration with the presence of vacuoles in addition to a shortening of the basal infoldings and basal deposits in aged APP/PS1 mice. These findings suggested that A $\beta$  deposition could cause a degenerative change in RPE in transgenic mouse. Previous studies have pointed out that A $\beta$  could induce oxidative stress in RPE cells<sup>[15]</sup> and in neurons<sup>[40]</sup>, and oxidative stresses were strongly related to RPE degeneration<sup>[41-42]</sup>. Therefore, oxidative stress might be a potential intermediate candidate that was responsible for the RPE degeneration observed in aged APP/PS1 mice. Recently, A $\beta$  had been reported to alter the expression of CRALBP and RPE65 in RPE both at the mRNA and protein levels<sup>[15,17]</sup>. CRALBP and RPE65 were two

important proteins in the visual cycle. These facts suggested that A $\beta$  might alter the functioning of the visual cycle, and photoreceptor homeostasis might be impacted due to the disturbance of visual cycle, and all of these insults might ultimately result in losses of the photoreceptor outer segments in mice, and this indication needed a further work to support. In order to phagocytose the debris of the outer segments, the vacuoles increasing in the RPE cells suggested by our performed experiments might due to the process of digesting the debris, a conclusion supported by our TEM characterization in which we found vacuoles containing membranous material in RPE cells.

Several studies have shown that A $\beta$  directly affected the tight junction and adhesion<sup>[43-44]</sup>. Furthermore, Bruban *et al*<sup>[15]</sup> have found that A $\beta$  caused the tight junction disruptions, as indicated by an increasing trans epithelial permeability in RPE cells in both *in vitro* and *in vivo* contexts. Our experiments have shown the RPE morphological changes with irregular shapes, which was further highlighted with the disorganization of ZO-1; taken together, these facts strongly suggested that A $\beta$  might be involved in modifying the tight junctions and cellular permeability in RPE cells, just as pointed out by another researcher<sup>[15]</sup>. In our work, however, there were no disruptions or missing segments of ZO-1 immunoreactivity in the borders of the RPE cells on the RPE flat mounts, indicating the possibility of undamaged RPE cells junctional integrity to some extent. The precise mechanisms relating to the observed A $\beta$ -induced tight junction disruptions still remain unknown.

As well-known, the presence of microglia infiltration plays a significant role in the inflammatory response caused by A $\beta$  deposition and in the clearance or turnover of A $\beta$  deposition in the brains of both humans and transgenic mice<sup>[40,45]</sup>. Microglia activation occurs early in the retina with retinal degeneration<sup>[46]</sup>. In AD transgenic mice, microglia cells infiltration has been detected coincidentally with the appearance of A $\beta$  deposition in the retinas<sup>[8-9,31]</sup>. In our experiments, we observed the accumulation of "dendritic-like" IBA-1 positive cells in the RPE layer on flat mounts in aged APP/PS1 mice. Considering IBA-1 as a microglia cell marker and that the location and appearance of these cells, we proposed they were microglia cells. Amazingly, we found that microglia cells were co-stained with A $\beta$  depositions on RPE flat mounts. Our work supported that microglia might migrate in response to A $\beta$  or A $\beta$ -induced inflammatory factors, such as chemokine monocyte chemoattractant protein-1 (MCP-1)<sup>[31]</sup>, and might interact with A $\beta$  in an internal attempt to remove it<sup>[47-48]</sup>. More interestingly, we found a significant increase in microglia/macrophages cells infiltration beneath the RPE layer in the immunofluorescence and TEM tests. This result appears difficult to explain. Although the number of microglia cells increased on the RPE layer surface in aged APP/PS1 mice, they may be less capable of clearing waste material

or A $\beta$  deposits and appeared overloaded with debris and A $\beta$  deposits<sup>[49]</sup>. As a result, more microglia cells were needed to be recruited in an attempt to maintain a homeostasis between the accumulation of A $\beta$  deposits or cellular debris and their clearance, as pointed out by Hoh Kam *et al*<sup>[14]</sup> in aged mice. The macrophages in choroid vessels, close to the RPE cell, would be perfect candidates for recruitment; however, if over-recruited, microglia cells might, in turn, caused RPE/BrM interface complex degeneration by inducing an inflammatory reaction<sup>[50]</sup>, which was supported by our findings of a thickened BrM and basal deposition in APP/PS1 mice. But we could not rule out the role that A $\beta$  direct toxicity played in RPE/BrM interface complex degeneration. Future studies should elucidate the relationship between microglia cells activation and RPE degeneration caused by A $\beta$  depositions.

In summary, the aged APP/PS1 mice investigated in this study demonstrated that A $\beta$  deposition might cause the RPE degeneration that is associated with microglia cell infiltration on RPE flat mounts, which suggests that A $\beta$  might play a critical role in RPE-related degenerative diseases, such as AMD.

#### ACKNOWLEDGEMENTS

**Authors' contributions:** Dong ZZ and Li J conceived of the study and experimental design and drafted manuscript. Dong ZZ and Li J carried out experiments. Gan YF, Sun XR and Leng YX helped experimental design, data analysis, and drafting manuscript. Dong ZZ initiated original idea for the study and steered data presentation and manuscript drafting and revision. Ge J and Li J funded the study, Ge J guided conceiving of the study and experiments, and helped data analysis, manuscript drafting and revision. All authors read and approved the final manuscript.

**Foundations:** Supported by the National Natural Science Foundation of China (No.81430009; No.81400424); the Science and Technology Research and Development Project of Shaanxi Province (No.2014K11-03-07-04).

**Conflicts of Interest:** Dong ZZ, None; Li J, None; Gan YF, None; Sun XR, None; Leng YX, None; Ge J, None.

#### REFERENCES

- 1 Roher AE, Kokjohn TA, Clarke SG, Sierks MR, Maarouf CL, Serrano GE, Sabbagh MS, Beach TG. APP/A $\beta$  structural diversity and Alzheimer's disease pathogenesis. *Neurochem Int* 2017;110:1-13.
- 2 Aisen PS, Cummings J, Jack CR Jr, Morris JC, Sperling R, Frölich L, Jones RW, Dowsett SA, Matthews BR, Raskin J, Scheltens P, Dubois B. On the path to 2025: understanding the Alzheimer's disease continuum. *Alzheimers Res Ther* 2017;9(1):60.
- 3 Mandrekar-Colucci S, Landreth GE. Microglia and inflammation in Alzheimer's disease. *CNS Neurol Disord Drug Targets* 2010;9(2):156-167.
- 4 Fernandez-Perez EJ, Peters C, Aguayo LG. Membrane damage induced by amyloid beta and a potential link with neuroinflammation. *Curr Pharm Des* 2016;22(10):1295-1304.
- 5 Majd S, Power JH, Grantham HJ. Neuronal response in Alzheimer's and Parkinson's disease: the effect of toxic proteins on intracellular pathways.

- BMC Neurosci* 2015;16:69.
- 6 Pogue AI, Dua P, Hill JM, Lukiw WJ. Progressive inflammatory pathology in the retina of aluminum-fed 5xFAD transgenic mice. *J Inorg Biochem* 2015;152:206-209.
- 7 Tsai Y, Lu B, Ljubimov AV, Girman S, Ross-Cisneros FN, Sadun AA, Svendsen CN, Cohen RM, Wang S. Ocular changes in TgF344-AD rat model of Alzheimer's disease. *Invest Ophthalmol Vis Sci* 2014;55(1):523-534.
- 8 Perez SE, Lumayag S, Kovacs B, Mufson EJ, Xu S. Beta-amyloid deposition and functional impairment in the retina of the APPswe/PS1DeltaE9 transgenic mouse model of Alzheimer's disease. *Invest Ophthalmol Vis Sci* 2009;50(2):793-800.
- 9 Liu B, Rasool S, Yang Z, Glabe CG, Schreiber SS, Ge J, Tan Z. Amyloid-peptide vaccinations reduce {beta}-amyloid plaques but exacerbate vascular deposition and inflammation in the retina of Alzheimer's transgenic mice. *Am J Pathol* 2009;175(5):2099-2110.
- 10 Bandello F, Sacconi R, Querques L, Corbelli E, Cicinelli MV, Querques G. Recent advances in the management of dry age-related macular degeneration: A review. *F1000Res* 2017;6:245.
- 11 Ferrington DA, Sinha D, Kaarniranta K. Defects in retinal pigment epithelial cell proteolysis and the pathology associated with age-related macular degeneration. *Prog Retin Eye Res* 2016;51:69-89.
- 12 Williams MA, Silvestri V, Craig D, Passmore AP, Silvestri G. The prevalence of age-related macular degeneration in Alzheimer's disease. *J Alzheimers Dis* 2014;42(3):909-914.
- 13 Koronyo Y, Salumbides BC, Black KL, Koronyo-Hamaoui M. Alzheimer's disease in the retina: imaging retinal a $\beta$  plaques for early diagnosis and therapy assessment. *Neurodegener Dis* 2012;10(1-4):285-293.
- 14 Hoh Kam J, Lenassi E, Jeffery G. Viewing ageing eyes: diverse sites of amyloid Beta accumulation in the ageing mouse retina and the up-regulation of macrophages. *PLoS One* 2010;5(10):e13127.
- 15 Bruban J, Glotin AL, Dinet V, Chalour N, Sennlaub F, Jonet L, An N, Faussat AM, Mascarelli F. Amyloid-beta(1-42) alters structure and function of retinal pigmented epithelial cells. *Aging Cell* 2009;8(2):162-177.
- 16 Liu C, Sun Z, Cao L, Wang F. Alterations of retinal tissue induced by amyloid  $\beta$ (1-42) subretinal injection in mice. *Zhonghua Yan Ke Za Zhi* 2015;51(11):831-838.
- 17 Yoshida T, Ohno-Matsui K, Ichinose S, Sato T, Iwata N, Saido TC, Hisatomi T, Mochizuki M, Morita I. The potential role of amyloid beta in the pathogenesis of age-related macular degeneration. *J Clin Invest* 2005;115(10):2793-2800.
- 18 Cao L, Wang H, Wang F, Xu D, Liu F, Liu C. A $\beta$ -induced senescent retinal pigment epithelial cells create a proinflammatory microenvironment in AMD. *Invest Ophthalmol Vis Sci* 2013;54(5):3738-3750.
- 19 Liu XC, Liu XF, Jian CX, Li CJ, He SZ. IL-33 is induced by amyloid- $\beta$  stimulation and regulates inflammatory cytokine production in retinal pigment epithelium cells. *Inflammation* 2012;35(2):776-784.
- 20 Lee CY, Landreth GE. The role of microglia in amyloid clearance from the AD brain. *J Neural Transm (Vienna)* 2010;117(8):949-960.
- 21 Aruoma OI, Jen SS, Watts HR, George J, Gentleman SM, Anderson PJ, Jen LS. Acute and chronic effects of intravitreally injected beta-amyloid on the neurotransmitter system in the retina. *Toxicology* 2009;256(1-2):92-100.

- 22 Luhmann UF, Robbie S, Munro PM, Barker SE, Duran Y, Luong V, Fitzke FW, Bainbridge JW, Ali RR, MacLaren RE. The drusenlike phenotype in aging Ccl2-knockout mice is caused by an accelerated accumulation of swollen autofluorescent subretinal macrophages. *Invest Ophthalmol Vis Sci* 2009;50(12):5934-5943.
- 23 Jankowsky JL, Slunt HH, Ratovitski T, Jenkins NA, Copeland NG, Borchelt DR. Co-expression of multiple transgenes in mouse CNS: a comparison of strategies. *Biomol Eng* 2001;17(6):157-165.
- 24 Praticò D, Uryu K, Leight S, Trojanowski JQ, Lee VM. Increased lipid peroxidation precedes amyloid plaque formation in an animal model of Alzheimer amyloidosis. *J Neurosci* 2001;21(12):4183-4187.
- 25 Zhang B, Veasey SC, Wood MA, Leng LZ, Kaminski C, Leight S, Abel T, Lee VM, Trojanowski JQ. Impaired rapid eye movement sleep in the Tg2576 APP murine model of Alzheimer's disease with injury to pedunculopontine cholinergic neurons. *Am J Pathol* 2005;167(5):1361-1369.
- 26 Li J, Dong Z, Liu B, Zhuo Y, Sun X, Yang Z, Ge J, Tan Z. Hypoxia induces beta-amyloid in association with death of RGC-5 cells in culture. *Biochem Biophys Res Commun* 2011;410(1):40-44.
- 27 Ding JD, Johnson LV, Herrmann R, Farsiu S, Smith SG, Groelle M, Mace BE, Sullivan P, Jamison JA, Kelly U, Harrabi O, Bollini SS, Dilley J, Kobayashi D, Kuang B, Li W, Pons J, Lin JC, Bowes Rickman C. Anti-amyloid therapy protects against retinal pigmented epithelium damage and vision loss in a model of age-related macular degeneration. *Proc Natl Acad Sci U S A* 2011;108(28):E279-E287.
- 28 Longbottom R, Fruttiger M, Douglas RH, Martinez-Barbera JP, Greenwood J, Moss SE. Genetic ablation of retinal pigment epithelial cells reveals the adaptive response of the epithelium and impact on photoreceptors. *Proc Natl Acad Sci U S A* 2009;106(44):18728-18733.
- 29 Behndig A. Corneal endothelial integrity in aging mice lacking superoxide dismutase-1 and/or superoxide dismutase-3. *Mol Vis* 2008;14:2025-2030.
- 30 Provost AC, Vede L, Bigot K, Keller N, Tailleur A, Jaïs JP, Savoldelli M, Ameqrane I, Lacassagne E, Legeais JM, Staels B, Menasche M, Mallat Z, Behar-Cohen F, Abitbol M. Morphologic and electroretinographic phenotype of SR-BI knockout mice after a long-term atherogenic diet. *Invest Ophthalmol Vis Sci* 2009;50(8):3931-3942.
- 31 Ning A, Cui J, To E, Ashe KH, Matsubara J. Amyloid-beta deposits lead to retinal degeneration in a mouse model of Alzheimer disease. *Invest Ophthalmol Vis Sci* 2008;49(11):5136-5143.
- 32 Fu X, Lin R, Qiu Y, Yu P, Lei B. Overexpression of angiotensin-converting enzyme 2 ameliorates amyloid  $\beta$ -induced inflammatory response in human primary retinal pigment epithelium. *Invest Ophthalmol Vis Sci* 2017;58(7):3018-3028.
- 33 Gupta VK, Chitranshi N, Gupta VB, Golzan M, Dheer Y, Wall RV, Georgevsky D, King AE, Vickers JC, Chung R, Graham S. Amyloid  $\beta$  accumulation and inner retinal degenerative changes in Alzheimer's disease transgenic mouse. *Neurosci Lett* 2016;623:52-56.
- 34 Georgiadis A, Tschernutter M, Bainbridge JW, Balaggan KS, Mowat F, West EL, Munro PM, Thrasher AJ, Matter K, Balda MS, Ali RR. The tight junction associated signalling proteins ZO-1 and ZONAB regulate retinal pigment epithelium homeostasis in mice. *PLoS One* 2010;5(12):e15730.
- 35 Volianskis A, Køstner R, Mølgaard M, Hass S, Jensen MS. Episodic memory deficits are not related to altered glutamatergic synaptic transmission and plasticity in the CA1 hippocampus of the APPswe/PS1 $\Delta$ E9-deleted transgenic mice model of  $\beta$ -amyloidosis. *Neurobiol Aging* 2010;31(7):1173-1187.
- 36 Sérière S, Tauber C, Vercouillie J, Mothes C, Pruckner C, Guilloteau D, Kassiou M, Doméné A, Garreau L, Page G, Chalon S. Amyloid load and translocator protein 18 kDa in APPswePS1- $\Delta$ E9 mice: a longitudinal study. *Neurobiol Aging* 2015;36(4):1639-1652.
- 37 Dutescu RM, Li QX, Crowston J, Masters CL, Baird PN, Culvenor JG. Amyloid precursor protein processing and retinal pathology in mouse models of Alzheimer's disease. *Graefes Arch Clin Exp Ophthalmol* 2009;247(9):1213-1221.
- 38 Johnson LV, Leitner WP, Rivest AJ, Staples MK, Radeke MJ, Anderson DH. The Alzheimer's A beta -peptide is deposited at sites of complement activation in pathologic deposits associated with aging and age-related macular degeneration. *Proc Natl Acad Sci U S A* 2002;99(18):11830-11835.
- 39 Koyama Y, Matsuzaki S, Gomi F, Yamada K, Katayama T, Sato K, Kumada T, Fukuda A, Matsuda S, Tano Y, Tohyama M. Induction of amyloid beta accumulation by ER calcium disruption and resultant upregulation of angiogenic factors in ARPE19 cells. *Invest Ophthalmol Vis Sci* 2008;49(6):2376-2383.
- 40 Serrano-Pozo A, Muzikansky A, Gómez-Isla T, Growdon JH, Betensky RA, Frosch MP, Hyman BT. Differential relationships of reactive astrocytes and microglia to fibrillar amyloid deposits in Alzheimer disease. *J Neuropathol Exp Neurol* 2013;72(6):462-471.
- 41 Datta S, Cano M, Ebrahimi K, Wang L, Handa JT. The impact of oxidative stress and inflammation on RPE degeneration in non-neovascular AMD. *Prog Retin Eye Res* 2017;60:201-218.
- 42 Hanus J, Anderson C, Wang S. RPE necroptosis in response to oxidative stress and in AMD. *Ageing Res Rev* 2015;24(Pt B):286-298.
- 43 Spampinato SF, Merlo S, Sano Y, Kanda T, Sortino MA. Astrocytes contribute to A $\beta$ -induced blood-brain barrier damage through activation of endothelial MMP9. *J Neurochem* 2017;142(3):464-477.
- 44 Gheorghiu M, Enciu AM, Popescu BO, Gheorghiu E. Functional and molecular characterization of the effect of amyloid- $\beta$ 42 on an in vitro epithelial barrier model. *J Alzheimers Dis* 2014;38(4):787-798.
- 45 Ruan L, Kang Z, Pei G, Le Y. Amyloid deposition and inflammation in APPswe/PS1 $\Delta$ E9 mouse model of Alzheimer's disease. *Curr Alzheimer Res* 2009;6(6):531-540.
- 46 Liu RT, Gao J, Cao S, Sandhu N, Cui JZ, Chou CL, Fang E, Matsubara JA. Inflammatory mediators induced by amyloid-beta in the retina and RPE in vivo: implications for inflammasome activation in age-related macular degeneration. *Invest Ophthalmol Vis Sci* 2013;54(3):2225-2237.
- 47 Doens D, Fernández PL. Microglia receptors and their implications in the response to amyloid  $\beta$  for Alzheimer's disease pathogenesis. *J Neuroinflammation* 2014;11:48.
- 48 Cai Z, Hussain MD, Yan LJ. Microglia, neuroinflammation, and beta-amyloid protein in Alzheimer's disease. *Int J Neurosci* 2014;124(5):307-321.
- 49 Xu H, Chen M, Manivannan A, Lois N, Forrester JV. Age-dependent accumulation of lipofuscin in perivascular and subretinal microglia in experimental mice. *Ageing Cell* 2008;7(1):58-68.
- 50 Ma W, Zhao L, Fontainhas AM, Fariss RN, Wong WT. Microglia in the mouse retina alter the structure and function of retinal pigmented epithelial cells: a potential cellular interaction relevant to AMD. *PLoS One* 2009;4(11):e7945.